**Contemporary Engineering Sciences, Vol. 9, 2016, no. 9, 425 - 442**
**HIKARI Ltd, www.m-hikari.com**
**http://dx.doi.org/10.12988/ces.2016.6216**

# Mathematical Modeling of the Guidance System of Satellite Antenna

**Sergei Evgenievich Ivanov**

ITMO National Research University (ITMO University)
Department of Information Systems
197101 Saint Petersburg, 49 Kronverksky Pr., Russian Federation

**Eugeny Petrovich Kolpak**

Saint Petersburg State University
Faculty of Applied Mathematics and Control Process
199034 Saint Petersburg, Universitetskaya nab., 7/9, Russian Federation



**Abstract**

The present paper develops a mathematical model of mobile satellite antenna elliptical shape which is under the influence of wind loads. The wind load is calculated in the framework of a hydrodynamic model for the mathematical package freeFEM++. To reduce the external impact, a model of vibration protection device is developed. The solution of developed mathematical model is constructed using numerical and analytical methods.

**Keywords**: mathematical modeling, satellite-offset antenna, mobile antenna, flow around the antenna, the guidance system of satellite antenna, device of vibration protection

## 1 Introduction

The system of receiving a signal from the satellite consists of a satellite antenna, part of which: a reflector, a receiver and converter [1, 2]. The elements of antenna are usually made of thin steel or aluminum. When external forces: wind, rain and snow loads in thin-walled components can be subjected to strong stress, resulting in local damage. The mobile antenna system is subjected to the periodic mechanical force effect during their movement. The antennas can be exposed to corrosive environments which cause corrosion and oxidation. To protect against the external aggressive environment is used special materials, coatings, protective equipment [3-7]. One of the main problems at the design stage is calculation of the strength of antenna elements. For mobile TV broadcasts are widely used system for automatic adjustment to a satellite the reflector of antenna [8, 9]. For mobile satellite systems is necessary to design an effective vibration protection system [10 – 14].

The most widely used offset ellipsoidal satellite antennas that have a number of advantages over other types of antennas.

Figure 1 shows a photograph of the offset satellite antenna.

For the antenna the reflected signal is focused below the center of the reflector, so the lift angle of the antenna to the satellite is small that allows almost vertical installation of the reflector.

Another advantage for offset antenna is constancy to signal reception, because installed below the converter does not close the reflector his shadow. For antennas with parabolic reflector is required a precise orientation to the selected satellite.

Fig.1 The offset satellite antenna

The manufacturers offset antennas are companies such as: Supral, Golden Interstar, Russat, Lans, Globo, Mabo, Triax, TracVision. For antennas, which are mounted on rail and sea transport are manufactured mobile satellite antenna small diameter. Stationary offset satellite antennas are typical characteristics: diameter reflector 80-100 cm, aluminum reflector material, the thickness of 1.1-1.4 mm, amplification coefficient 38-40 dB, weight 4-5 kg. Small mobile satellite antennas have typical characteristics: diameter reflector 45-60 cm, thickness 1.1-1.4 mm, amplification coefficient 46-48 dB, weight 10-15 kg.

## 2 The definition of wind pressure on the reflector and the protective dome for satellite antenna

The pressure of air flow is considered to be potential.

The components of air velocity $\mathbf{v}$ are associated with the potential of $\psi$ the following equation: $\mathbf{v} = grad\ \psi$ . (1)

The velocity potential satisfies the equation: $\Delta\psi = 0$.

We assume that the antenna is impervious to air flow. Therefore, on the surface of the antenna must meet the following condition: $\left.\frac{\partial\psi}{\partial n}\right|_S = 0$.

We assume that the antenna at a sufficient distance from it does not introduce perturbations in air traffic. Accordingly, we assume that at infinity the velocity vector components are constant and the direction of air flow is directed at an angle 0,45,90,135,180,225,270,315,360 degrees.

To solve the Laplace equation the condition at infinity, we replace the condition on the large radius of the circle: $R >> R_{antena}$, $\psi|_\infty = \psi|_{R^2}$

For find the pressure are using the Bernoulli equation to compressible gas in the form: $\rho\frac{v^2}{2} + \rho gh + \frac{\gamma}{\gamma - 1} p = const$, (2)

where $p$ - the pressure of the gas, $\rho$ - the density of the gas, $\gamma$ - the adiabatic constant of the gas, $v$ - the speed the incoming flow, $h$ - the height of the installation, $g$ - the acceleration of free fall. The numerical solution of the problem is made in the mathematical package freeFEM ++ [15].

We have constructed the grid model in the field of circle large-radius (Figure 2).

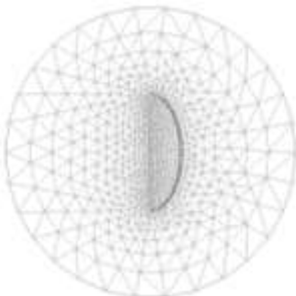

Fig.2 The grid model the flow around the antenna reflector

We carried out simulation of flow around the satellite antenna in the two-dimensional case for the eight directions of the flux vector. Figure 3 shows the flow line an angle of 45 degrees.

Fig.3 the flow function lines at an angle of 45 degrees

Fig. 4 shows a velocity vector field at an angle of 0 degrees. The arrows indicate the direction of flow.

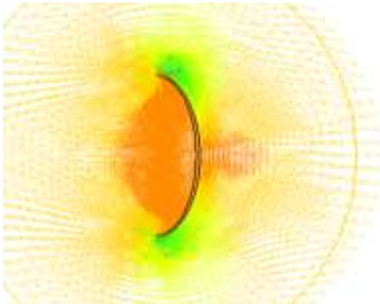

Fig.4 The vector field of velocity for the stream at an angle of 0 degrees

Fig. 5 shows the pressure contour at an angle of 45 degrees.

Fig.5 The lines of the pressure contour at an angle of 45 degrees

We carried out simulation of wind pressure, depending on the elliptical shape offset satellite antenna with radius of reflector: 100x110, 100x130, 100x150 cm.
Horizontal and vertical semi-axes of the ellipse of the reflector are denoted: $R_x, R_y$
Fig. 6 shows the dependence of the wind pressure to the size of the reflector antenna, the magnitude of semi-axes $R_x$ at the following ratios of the semi-axes: $R_y = 1.1R_x$ -gray graph, $R_y = 1.3R_x$ -green graph, $R_y = 1.5R_x$ -blue graph and the maximum wind speed $v = 30$

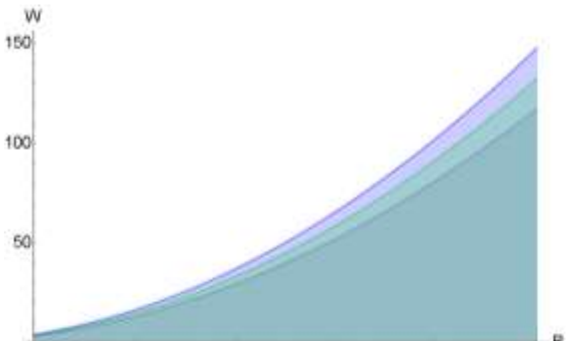


Fig.6 The dependence of the wind pressure to the length of semi-axes reflector

Figure 7 shows the dependence of the wind pressure on the wind speed, taking into account the fluctuating component in the following sizes offset satellite antennas: $a = 0.5, b = 0.55$ -blue graph, $a = 1, b = 1.1$ -green graph, $a = 2, b = 2.2$ -yellow graph.

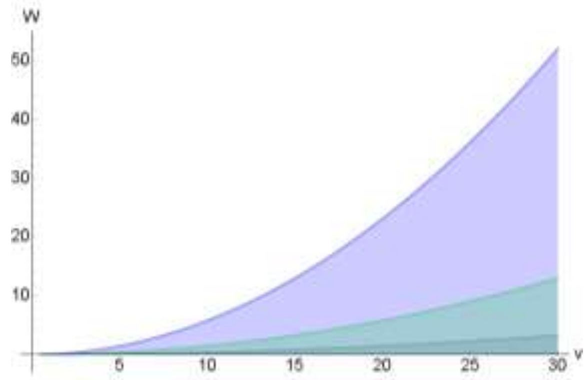


Fig.7 The dependence of the wind pressure on the wind speed

For protection against the external impacts and improving aerodynamics the mobile satellite antennas to installing on the sea and railway transport are covered the spherical dome (Figure 8).

Fig.8 Dome for the protection satellite antenna.

The dome to protect the satellite antenna is made of thin plastic radius of 60-80 cm. We assume that the contour of the dome is impervious to air flow and the flow velocity at infinity is constant and directed parallel to the vector flow. The components of the flow velocity at infinity are constant. Fig. 9 shows velocity vector field at an angle of 0 degrees indicate the direction of flow.

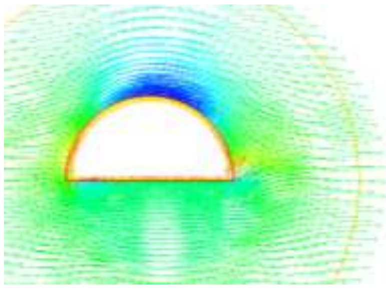

Fig.9 The vector field of velocity for the stream at an angle of 0 degrees

Fig. 10 shows the pressure contour at an angle of 45 degrees.

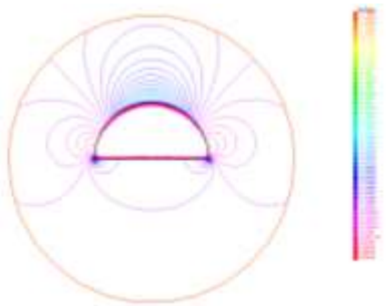

Fig.10 The lines of the pressure contour at an angle of 0 degrees

Figure 11 shows the depending the wind pressure to the radius of the reflector (green graph), of the protective dome (blue graph).

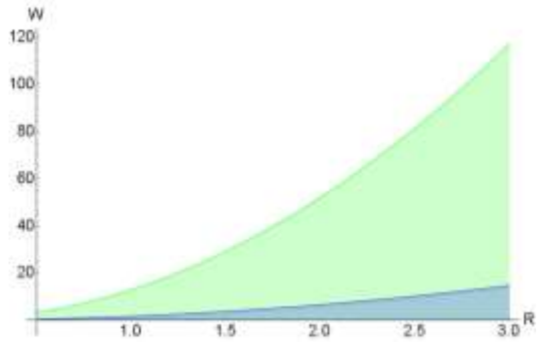


Fig.11 The dependence of the wind pressure on the radius of the reflector.

The comparing the function of pressure for the reflector and the protective dome antenna is shows the reduction in the maximum wind pressure is more than ten times when using the dome for the satellite antenna.

## 3 The mathematical modeling of the mechanical guidance system to satellite in view of wind pressure

For automatic guidance to satellite of the reflector of mobile antenna is used articulated mechanical system allowing to fold the antenna for transport and rotate the antenna in two orthogonal planes.
A mechanical guidance system in the mobile satellite antenna has three degrees of freedom. Figure 12 shows the mechanical guidance system to satellite mobile antenna.

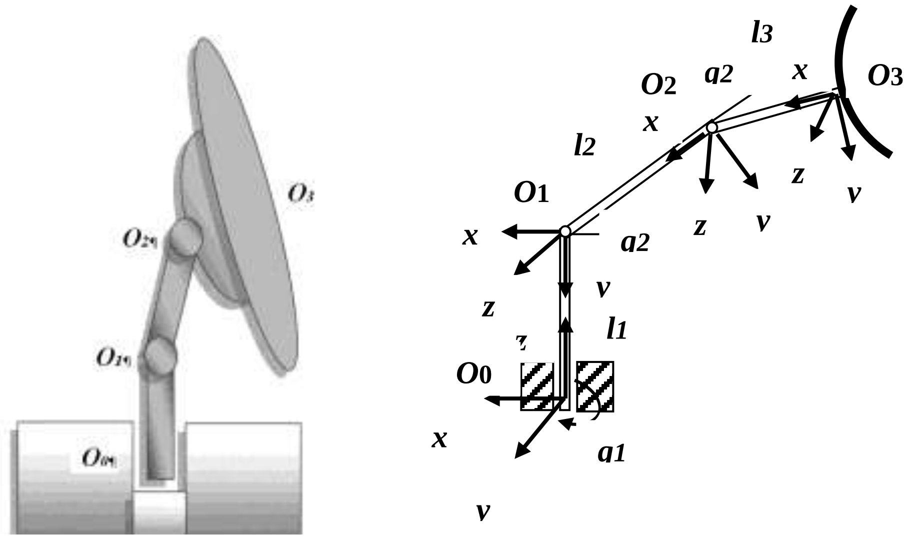


Fig.12 The mechanical guidance system to satellite and kinematic diagram

The mechanical system includes three parts (Fig. 12), the length each equal $l_1, l_2, l_3$ respectively. The three parts are rotated in a plane.

We introduce the relative reference system associated with the parts, with its origin at the points: $O_1, O_2, O_3$. The initial system of reference $O_0$ associate with a movable object on which the antenna is installed. The rotation angles in the planes we choose for the generalized coordinates of the system: $q_1, q_2, q_3$

We developed the system of dynamic equations of motion of the antenna, taking into account wind pressure. We applied the matrix method and dynamic Lagrange equations in matrix form to produce the equations of motion [16 – 17].

The transition from the coordinate system $O_0$ to $O_1$ occurs by rotation around the z-axis at an angle $q_1$, by shift along the z-axis on $l_1$, rotation about the x-axis and an angle $-\pi/2$. The transition from the coordinate system $O_1$ to $O_2$ occurs by rotation around the z-axis at an angle $q_2$ and by shift along the x-axis on $-l_2$.

The transition from the coordinate system $O_2$ to $O_3$ occurs by rotation around the z-axis at an angle $q_3$ and by shift along the x-axis on $-l_3$.

We introduce the radius vector of points in the local coordinate system $O_i$.

$R_i = \begin{bmatrix} x_i & y_i & z_i & 1 \end{bmatrix}^T$ .

The communication the radius vectors in the coordinate system $O_{i-1}$ and $O_i$ by using the transition matrix $A_i$ : $R_{i-1} = A_i R_i$

The transition matrix from $O_0$ to $O_1$ and transition matrix from $O_1$ to $O_2$

$$A_1 = \begin{pmatrix} \cos(q_1) & 0 & -\sin(q_1) & 0 \\ \sin(q_1) & 0 & \cos(q_1) & 0 \\ 0 & -1 & 0 & l_1 \\ 0 & 0 & 0 & 1 \end{pmatrix} A_2 = \begin{pmatrix} \cos(q_2) & -\sin(q_2) & 0 & -l_2\cos(q_2) \\ \sin(q_2) & \cos(q_2) & 0 & -l_2\sin(q_2) \\ 0 & 0 & 1 & 0 \\ 0 & 0 & 0 & 1 \end{pmatrix}$$

The transition matrix from $O_2$ to $O_3$

$$A_3 = \begin{pmatrix} \cos(q_3) & -\sin(q_3) & 0 & -l_3\cos(q_3) \\ \sin(q_3) & \cos(q_3) & 0 & -l_3\sin(q_3) \\ 0 & 0 & 1 & 0 \\ 0 & 0 & 0 & 1 \end{pmatrix}$$

The transition matrix $A_{02}$ from $O_0$ to $O_2$ is defined as the product of the matrices $A_1A_2 = A_{02}$, and transition matrix $A_{03}$ from $O_0$ to $O_3$ is obtained by multiplying matrices $A_1A_2A_3 = A_{03}$

We calculated the kinetic energy of each unit and the total energy.

For determine of kinetic energy the part we use the matrix formula with the transition matrices:

$$T_i = \frac{1}{2} tr(\dot{\mathrm{A}}_{0i}\mathrm{H}_i\dot{\mathrm{A}}_{0i}^T) \tag{3}$$

$\mathrm{H}_i$ - inertia matrix of part $i$

$$\mathrm{H}_i = \begin{bmatrix} J_{xxi} & J_{xyi} & J_{xzi} & m_ix_i \\ J_{yxi} & J_{yyi} & J_{yzi} & m_iy_i \\ J_{zxi} & J_{zyi} & J_{zzi} & m_iz_i \\ m_ix_i & m_iy_i & m_iz_i & m_i \end{bmatrix}$$

Here $m_1, m_2, m_3$ - mass of parts. Coordinates of the center of gravity part in the local coordinate system are designated: $x_i, y_i, z_i$. $J_{xxi}, J_{yyi}, J_{zzi}$ - the elements of the inertia tensor of part *i* a relatively their own axes.

The moments of inertia of part *i* about the axis am denoted: $J_{xi}, J_{yi}, J_{zi}$

We define the kinetic energy of the parts in the matrix equation (3) with the equations: $J_{yyi}+J_{zzi} = J_{xi}, J_{xxi}+J_{zzi} = J_{yi}, J_{xxi}+J_{yyi} = J_{zi}$.

The kinetic energy ($T_1, T_2, T_3$) of the first, second and third part we calculate by formulas: $T_1 = 0.5J_{y1}q_1'(t)^2$,

$$T_2 = \dot{q}_1^2\left(J_{x2}(0.25\text{-}0.25(\cos(2(q_2)))) + J_{y2}(0.25\cos(2(q_2)) + 0.25)\right) +$$
$$0.5J_{z2}\dot{q}_2^2 + l_2^2 m_2\left(0.25\dot{q}_1^2(\cos(2(q_2))) + 0.25\dot{q}_1^2 + 0.5\dot{q}_2^2\right),$$
$$T_3 = \dot{q}_1^2\left(J_{x3}(0.25\text{-}0.25(\cos(2t(q_2+q_3)))) + J_{y3}(0.25\cos(2t(q_2+q_3)) + 0.25)\right) +$$
$$m_3 l_3\left(l_2(\cos(tq_3))\left(0.5\dot{q}_1^2 + \dot{q}_2^2\right) + \dot{q}_1^2\left(0.5l_2(\cos(2q_2t + q_3t)) + 0.25l_3(\cos(2(q_2t + q_3t)))\right)\right) +$$
$$m_3\left(0.25l_2^2\dot{q}_1^2(\cos(2(q_2t))) + \left(l_2^2 + l_3^2\right)\dot{q}_1^2/4 + \left(l_2^2 + l_3^2\right)\dot{q}_2^2/2 + l_3^2\dot{q}_3^2/2\right) + J_{z3}\left(\dot{q}_2^2 + \dot{q}_3^2\right)/2$$

The total kinetic energy $T$ is equal to the sum of the kinetic energies of the three parts: $T = T_1 + T_2 + T_3$

We calculate the potential energy of each part and the total energy.
In matrix form, the potential energy part takes the form:

$$P_i = -m_i G^T A_i R_i \qquad (4)$$

Here $R_i = \begin{bmatrix} x_i & y_i & z_i & 1 \end{bmatrix}^T$ - column-matrix of the coordinates of the center of gravity part

$G_i^T = \begin{bmatrix} 0 & 0 & -g & 0 \end{bmatrix}$ - row-matrix for the acceleration of free fall

The total potential energy is calculated by formula:

$$P = gm_3\left(l_3\sin(q2)\cos(q3) + l_3\cos(q2)\sin(q3) + l_2\sin(q2) + l_1\right) +$$
$$+gm_2\left(l_2\sin(q2) + l_1\right) + gl_1m_1$$

We apply Lagrange equations in matrix form for the equations of motion.

$$\frac{d}{dt}\frac{\partial T}{\partial \dot{q}_i} - \frac{\partial T}{\partial q_i} + \frac{\partial P}{\partial q_i} = Q_i \qquad (5)$$

Here $Q_1, Q_2, Q_3$ - generalized forces parts.

We denote the generalized forces generated electromotive of part which performs its rotation by a predetermined angle: $F_1, F_2, F_3$. The maximum wind pressure acting on the antenna reflector - the third part is denoted: $F_W$

We substitute the kinetic energy, potential energy and the generalized forces in the matrix of the Lagrange equation and obtain a system of equations of motion of the device with three degrees of freedom:

$$\ddot{q}_2\left(J_{z2} + J_{z3} + m_3\left(2l_3l_2(\cos(q_3)) + l_2^2 + l_3^2\right) + l_2^2m_2\right)\text{-}$$
$$+0.5J_{x3}\dot{q}_1^2(\sin(2(q_2+q_3))) + 0.5J_{y3}\dot{q}_1^2(\sin(2(q_2+q_3)))\text{ - }0.5J_{x2}\dot{q}_1^2(\sin(2(q_2))) +$$
$$+0.5J_{y2}\dot{q}_1^2(\sin(2(q_2))) + 0.5l_3^2m_3\dot{q}_1^2(\sin(2(q_2+q_3))) + l_2l_3m_3\dot{q}_1^2(\sin(2q_2+q_3)) +$$
$$+0.5l_2^2m_2\dot{q}_1^2(\sin(2(q_2))) + 0.5l_2^2m_3\dot{q}_1^2(\sin(2(q_2)))\text{ - }2l_2l_3m_3\dot{q}_2\dot{q}_3(\sin(q_3)) = F_2,$$

$$
\begin{aligned}
&\ddot{q}_1(J_{x3}\left(0.5-\cos\left(2\left(q_2+q_3\right)\right)/2\right)+J_{y3}\left(\cos\left(2\left(q_2+q_3\right)\right)/2+0.5\right)+\\
&J_{y2}\left(\cos\left(2q_2\right)/2+0.5\right)+J_{y1}+l_2^2m_2(\cos(2(q_2))/2+0.5)+m_3l_2^2(\cos(2(q_2))/2+0.5)+\\
&m_3\left(l_3l_2(\cos(2q_2+q_3)+\cos(q_3))+l_3^2(0.5\cos(2(q_2+q_3))+0.5)\right)+\\
&J_{x2}\left(\ddot{q}_1(0.5-0.5(\cos(2(q_2))))+\dot{q}_1\dot{q}_2(\sin(2(q_2)))\right)+\\
&\dot{q}_1\left(\dot{q}_2\left((\sin(2(q_2+q_3)))\left(J_{x3}-J_{y3}-l_3^2m_3\right)-J_{y2}(\sin(2(q_2)))+\right)+\right.\\
&\dot{q}_1\left(\dot{q}_2\left(l_2\left(l_2\left(-m_2-m_3\right)(\sin(2(q_2)))-2l_3m_3(\sin(2q_2+q_3))\right)\right)\right)+\\
&\dot{q}_3\left((\sin(2(q_2+q_3)))\left(J_{x3}-J_{y3}-l_3^2m_3\right)+l_2l_3m_3(-(\sin(2q_2+q_3))-(\sin(q_3)))\right)\Big)=F_1,\\
&J_{z3}\ddot{q}_3+0.5J_{x3}\dot{q}_1^2(\sin(2(q_2+q_3)))+0.5J_{y3}\dot{q}_1^2(\sin(2(q_2+q_3)))+\\
&l_3m_3\left(l_2\left(\dot{q}_1^2(0.5\sin(2q_2+q_3)+0.5\sin(q3))+\dot{q}_2^2(\sin(q_3))\right)\right)+\\
&l_3^2m_3\left(0.5\dot{q}_1^2(\sin(2(q_2+q_3)))+\ddot{q}_3\right)=F_3+F_W
\end{aligned}
\tag{6}
$$

The solution of the nonlinear system of equations (6) is a numerical method of Runge-Kutta fourth-order with the following parameters of system:
$(l_1=0.5)(l_2=0.5)(l_3=0.1)(m_1=10)(m_2=5)(m_3=30)$

Figure 13 shows graphs of the dynamics of the corners - the generalized coordinates $q_1,q_2,q_3$ (blue, green and yellow graphic) while ensuring electric drive of parts the specified generalized forces: $F_1=0.01, F_2=0.01, F_3=0.01$, taking into account wind pressure $F_W=10$.

The initial position of the device is specified coordinates and velocities at the initial time: $q_1(0)=0, q_2(0)=\pi/2, q_3(0)=-\pi/2, \dot{q}_1(0)=0, \dot{q}_2(0)=0, \dot{q}_3(0)=0$

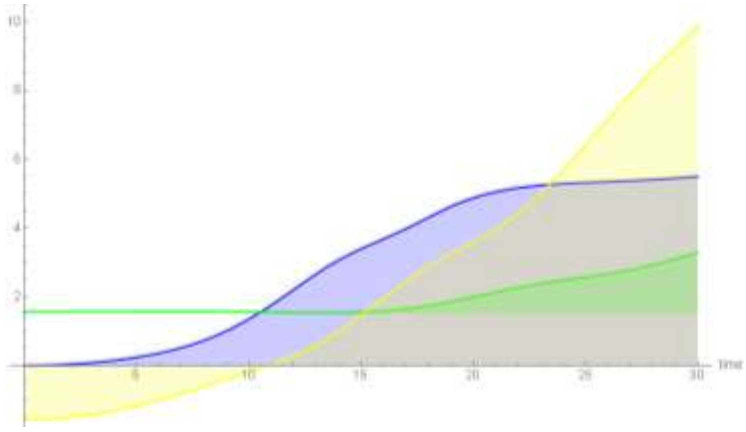

Fig.13 The dynamics of the generalized coordinates $q_1,q_2,q_3$

After receiving graphics dynamics corners of device can be determined how much time is necessary to work electric actuators of parts that generate a given constant force for parts, to ensure the necessary settings angles to the satellite reflector antennas.

## 4 The mathematical modeling of vibration protection device of mobile satellite antenna with the wind pressure

For protection from external vibrations mobile satellite antenna is mounted on device with non-linear damping characteristics (Fig 14).

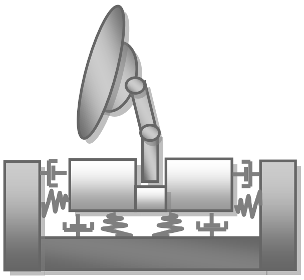

Fig.14 The scheme vibration protection device

The nonlinear characteristics of springs and dampers, we approximate the polynomial of the fifth degree.

The external impact generated when movement of transport on the satellite antenna we present a periodic force with a small $A, B$ amplitude and $\omega$ frequency: $f(t) = A\sin(\omega t) + B\cos(\omega t)$

For the equations of motion, we apply the Lagrange equation

$$\frac{d}{dt}\left(\frac{\partial L}{\partial \dot{x}}\right) - \frac{\partial L}{\partial x} = Q_x, \frac{d}{dt}\left(\frac{\partial L}{\partial \dot{y}}\right) - \frac{\partial L}{\partial y} = Q_y, \frac{d}{dt}\left(\frac{\partial L}{\partial \dot{z}}\right) - \frac{\partial L}{\partial z} = Q_z.$$

Here x, y, z coordinates of the center of gravity of the antenna device and the vibration isolation platform.

The total weight of the antenna consists of a mass of three parts $m_1, m_2, m_3$ and $m_p$ - weight of platform with a damping device: $m = m_1 + m_2 + m_3 + m_p$

By matrix methods, we determine the coordinates of the center of gravity of the antenna as a function of the generalized coordinates $q_1, q_2, q_3$:

$$x = \frac{m_3}{m}\begin{pmatrix} -l_3\cos(q_1)\cos(q_2)\cos(q_3) + l_3\cos(q_1)\sin(q_2)\sin(q_3) + l_2(-\cos(q_1))\cos(q_2) + \\ x_0(\cos(q_1)\cos(q_2)\cos(q_3) - \cos(q_1)\sin(q_2)\sin(q_3)) + \\ y_0(-\cos(q_1)\sin(q_2)\cos(q_3) - \cos(q_1)\cos(q_2)\sin(q_3)) - z_0\sin(q_1) \end{pmatrix} +$$

$$+m_2\left(-0.5l_2\cos(q_1)\cos(q_2) + x_0\cos(q_1)\cos(q_2) - y_0\cos(q_1)\sin(q_2) - z_0\sin(q_1)\right)/m +$$

$$+m_1\left(x_0\cos(q_1) - z_0\sin(q_1)\right)/m + m_p x_0 / \text{m},$$

$$y = \frac{m_3}{m}\begin{pmatrix} l_3\sin(q_1)\sin(q_2)\sin(q_3) - l_3\sin(q_1)\cos(q_2)\cos(q_3) + \\ l_2\sin(q_1)(-\cos(q_2)) + x_0(\sin(q_1)\cos(q_2)\cos(q_3) - \sin(q_1)\sin(q_2)\sin(q_3)) + \\ y_0(\sin(q_1)\sin(q_2)(-\cos(q_3)) - \sin(q_1)\cos(q_2)\sin(q_3)) + z_0\cos(q_1) \end{pmatrix} +$$

$$+m_2\left(-0.5l_2\sin(q_1)\cos(q_2) + x_0\sin(q_1)\cos(q_2) - y_0\sin(q_1)\sin(q_2) + z_0\cos(q_1)\right)/m +$$

$$+m_1\left(x_0\sin(q_1) + z_0\cos(q_1)\right)/m + m_p y_0 / \text{m},$$

$$z = \frac{m_3}{m}\begin{pmatrix} l_3\sin(q_2)\cos(q_3) + l_3\cos(q_2)\sin(q_3) + l_2\sin(q_2) + l_1 + \\ x_0(\sin(q_2)(-\cos(q_3)) - \cos(q_2)\sin(q_3)) + y_0(\sin(q_2)\sin(q_3) - \cos(q_2)\cos(q_3)) \end{pmatrix} +$$

$$+\frac{m_2}{m} + \left(\frac{1}{2}l_2\sin(q_2) + l_1 - x_0\sin(q_2) - y_0\cos(q_2)\right) + \frac{m_1}{m}\left(\frac{l_1}{2} - y_0\right) + \frac{m_p}{m}z_0.$$

We write the generalized force, taking into account wind pressure:

$$Q_x = w_x - b_1(\dot{x} - \dot{f}_x) - b_2(\dot{x} - \dot{f}_x)^2 - b_3(\dot{x} - \dot{f}_x)^3 - b_4(\dot{x} - \dot{f}_x)^4 - b_5(\dot{x} - \dot{f}_x)^5,$$

$$Q_y = w_y - b_6(\dot{y} - \dot{f}_y) - b_7(\dot{y} - \dot{f}_y)^2 - b_8(\dot{y} - \dot{f}_y)^3 - b_9(\dot{y} - \dot{f}_y)^4 - b_{10}(\dot{y} - \dot{f}_y)^5,$$

$$Q_z = w_z - b_{11}(\dot{z} - \dot{f}_z) - b_{12}(\dot{z} - \dot{f}_z)^2 - b_{13}(\dot{z} - \dot{f}_z)^3 - b_{14}(\dot{z} - \dot{f}_z)^4 - b_{15}(\dot{z} - \dot{f}_z)^5,$$

Here $b_i$ - damping coefficients, $c_i$ - spring stiffness, $w_x, w_y, w_z$ - components of the maximum wind pressure on the reflector.

We write a non-linear system of differential equations in relative coordinates transport: $x = \tilde{x} - f_x, y = \tilde{y} - f_y, z = \tilde{z} - f_z$

$$\begin{cases} m\ddot{x} + b_1\dot{x} + b_2\dot{x}^2 + b_3\dot{x}^3 + b_4\dot{x}^4 + b_5\dot{x}^5 + c_1x + c_2x^2 + c_3x^3 + c_4x^4 + c_5x^5 = \\ = w_x + m\omega^2A_1\sin(t\omega) + m\omega^2B_1\cos(t\omega) \\ my + b_6\dot{y} + b_7\dot{y}^2 + b_8\dot{y}^3 + b_9\dot{y}^4 + b_{10}\dot{y}^5 + c_6y + c_7y^2 + c_8y^3 + c_9y^4 + c_{10}y^5 = \\ = w_y + m\omega^2A_2\sin(t\omega) + m\omega^2B_2\cos(t\omega) \\ m\ddot{x} + b_{11}\dot{z} + b_{12}\dot{z}^2 + b_{13}\dot{z}^3 + b_{14}\dot{z}^4 + b_{15}\dot{z}^5 + c_{11}z + c_{12}z^2 + c_{13}z^3 + c_{14}z^4 + c_{15}z^5 = \\ = w_z + m\omega^2A_3\sin(t\omega) + m\omega^2B_3\cos(t\omega) \end{cases} \quad (7)$$

The solution of nonlinear differential equations [18-25] can be carried out various approximate analytical methods [26-35]: the method of Van der Pol, the harmonic balance method, the averaging method, the small parameter method, the method of Krylov-Bogolyubov, method of harmonic linearization, the method of Poincare.

We obtained an approximate analytical solution of the modified method of harmonic linearization with Chebyshev polynomials [36-42] under conditions: $A_1^2 + B_1^2 \le 1, A_2^2 + B_2^2 \le 1, A_3^2 + B_3^2 \le 1$

$$x(t)=\sin(t\omega_1)M_1N_1\left(A_1\omega_1^2N_1-8A_1\omega_1^4+\frac{5b_5B_1F_1^4\omega_1^7}{m}+\frac{6b_3B_1F_1^2\omega_1^5}{m}+\frac{8b_1B_1\omega_1^3}{m}\right)+$$

$$\cos(t\omega_1)M_1N_1\left(B_1\omega_1^2N_1-8B_1\omega_1^4-\frac{5A_1b_5F_1^4\omega_1^7}{m}-\frac{6A_1b_3F_1^2\omega_1^5}{m}-\frac{8A_1b_1\omega_1^3}{m}\right)-M_1b_1^2\omega_1^2w_x,$$

$$F_1^2\equiv A_1^2\omega_1^4+B_1^2\omega_1^4;M_1=m/\left(64c_1\left(b_1^2\omega_1^2/m^2+\left(c_1/m-\omega_1^2\right)^2\right)\right);$$

$$N_1=\left(F_1^2\left(5c_5F_1^2+6c_3\right)+8c_1\right)/m$$

$$y(t)=\sin(t\omega_2)M_2N_2\left(A_2\omega_2^2N_2-8A_2\omega_2^4+\frac{5b_{10}B_2F_2^4\omega_2^7}{m}+\frac{6b_8B_2F_2^2\omega_2^5}{m}+\frac{8b_6B_2\omega_2^3}{m}\right)+$$

$$\cos(t\omega_2)M_2N_2\left(B_2\omega_2^2N_2-8B_2\omega_2^4-\frac{5A_2b_{10}F_2^4\omega_2^7}{m}-\frac{6A_2b_8F_2^2\omega_2^5}{m}-\frac{8A_2b_6\omega_2^3}{m}\right)-M_2b_6^2\omega_2^2w_y,$$

$$F_2^2\equiv A_2^2\omega_2^4+B_2^2\omega_2^4;M_2=m/\left(64c_6\left(b_6^2\omega_2^2/m^2+\left(c_6/m-\omega_2^2\right)^2\right)\right);,$$

$$N_2=\left(F_2^2\left(5c_{10}F_2^2+6c_8\right)+8c_6\right)/m$$

$$z(t)=\sin(t\omega_3)M_3N_3\left(A_3\omega_3^2N_3-8A_3\omega_3^4+\frac{5b_{15}B_3F_3^4\omega_3^7}{m}+\frac{6b_{13}B_3F_3^2\omega_3^5}{m}+\frac{8b_{11}B_3\omega_3^3}{m}\right)+$$

$$\cos(t\omega_3)M_3N_3\left(B_3\omega_3^2N_3-8B_3\omega_3^4-\frac{5A_3b_{15}F_3^4\omega_3^7}{m}-\frac{6A_3b_{13}F_3^2\omega_3^5}{m}-\frac{8A_3b_{11}\omega_3^3}{m}\right)-M_3b_{11}^2\omega_3^2w_z,$$

$$F_3^2\equiv A_3^2\omega_3^4+B_3^2\omega_3^4;M_3=m/\left(64c_{11}\left(b_{11}^2\omega_3^2/m^2+\left(c_{11}/m-\omega_3^2\right)^2\right)\right);.$$

$$N_3=\left(F_3^2\left(5c_{15}F_3^2+6c_{13}\right)+8c_{11}\right)/m$$

We obtained modes of oscillation the mobile satellite antenna mounted on the damping device at the given parameters:

$$A_1=0.4;B_1=0.2;A_2=0.4;B_2=0.2;A_3=0.4;B_3=0.2;\omega_1=1;\omega_2=1;\omega_3=1;m=30;$$
$$b_1=0.2;b_2=0.1;b_3=0.1;b_4=0.1;b_5=0.1;b_6=0.2;b_7=0.1;b_8=0.1;b_9=0.1;b_{10}=0.1;$$
$$b_{11}=0.2;b_{12}=b_{13}=b_{14}=b_{15}=0.1;\ c_{11}=0.5;c_{12}=c_{13}=c_{14}=c_{15}=0.1;$$
$$c_1=0.5;c_2=0.1;c_3=0.1;c_4=0.1;c_5=0.1;c_6=0.5;c_7=0.1;c_8=0.1;c_9=0.1;c_{10}=0.1;$$
$$x(t)=-0.0181526\sin(t)-0.0128475\cos(t)$$
$$y(t)=-0.0191959\sin(t)-0.0134779\cos(t)$$
$$z(t)=-0.0205358\sin(t)-0.0148453\cos(t)$$

Figure 15 shows graphs of the vertical oscillations of mobile satellite antenna obtained by analytical method (blue), a numerical method (yellow) and the graph the oscillation without vibration protection devices (green).

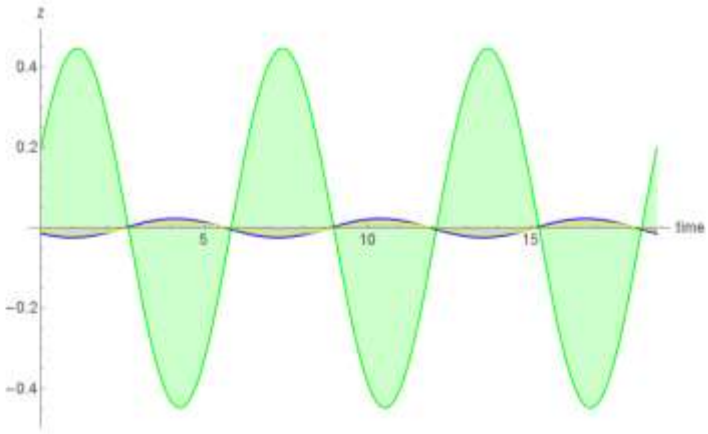


Fig.15 The vertical vibrations with vibration isolation device and without it

The graphs show the reduction of external periodic influence is 10 times when using vibration protection device.

## Conclusion

A simulation analysis of the results showed that the protection of offset antennas from external influences can provide a significant reduction in wind pressure and ensure the accuracy guidance of the antenna to satellite. The reduction of vibrations occurring when moving the mobile antenna can be achieved by creating an efficient vibration protection system. We developed the mathematical model that takes into account external load, which can be used in the management of the satellite antenna.

This work was supported by the Russian Foundation for Basic Research (Grant No. 16-08-00890).

## References

[1] A. Cepe, A. V. Kozlov, A. A. Nikulin, A problem of satellite orientation determination by spaced satellite antennas and angular rate sensors, *Journal of Computer and Systems Sciences International*, **54** (2015), no. 4, 651 - 655. http://dx.doi.org/10.1134/s1064230715030053

[2] J. Janetstephy, A. Anusuya, G. Jegan, Design and analysis of frequency reconfigurable micro strip patch antena for wireless applications, *International Journal of Applied Engineering Research*, **10** (2015), no. 6, 15899 - 15904.

[3] Y. G. Pronina, O. S. Sedova, S. A. Kabrits, On the applicability of thin

spherical shell model for the problems of mechanochemical corrosion, *AIP Conference Proceedings*, **1648** (2015).
http://dx.doi.org/10.1063/1.4912550

[4] Y. G. Pronina, Olga S. Sedova, Taking account of hydrostatic pressure in the modeling of corrosion of thick spherical shells, *2015 International Conference on Mechanics - Seventh Polyakhov's Reading*, (2015), 1 - 4.
http://dx.doi.org/10.1109/polyakhov.2015.7106771

[5] O. S. Sedova, L. A. Khaknazarova, Y. G. Pronina, Stress concentration near the corrosion pit on the outer surface of a thick spherical member, *10th International Vacuum Electron Sources Conference, IVESC 2014 and 2nd International Conference on Emission Electronics, ICEE,* (2014), 1 - 2.
http://dx.doi.org/10.1109/IVESC.2014.6892074

[6] O. S. Sedova, Y. G. Pronina, Initial boundary value problems for mechanochemical corrosion of a thick spherical member in terms of principal stress, *AIP Conference Proceedings*, **1648** (2015).
http://dx.doi.org/10.1063/1.4912519

[7] Y. G. Pronina, Thermoelastic stress analysis for a tube under general mechanochemical corrosion conditions, *Proceedings of the 4th International Conference on Computational Methods for Coupled Problems in Science and Engineering, COUPLED PROBLEMS 2011*, (2011), 1408 - 1415.

[8] M. N. Smirnov, M. A Smirnova, N. V. Smirnov, The method of accounting of bounded external disturbances for the synthesis of feedbacks with multi-purpose structure, *Lecture Notes in Engineering and Computer Science*, **2209** (2014), 301 - 304.

[9] Y. B. Mindlin, E. P. Kolpak, N. A. Gasratova, Clusters in system of instruments of territorial development of the Russian Federation, *International Review of Management and Marketing*, **6** (2016), 245 - 249.

[10] V. V. Dikusar, A. V. Zubov, N. V. Zubov, Structural minimization of stationary control and observation systems, *Journal of Computer and Systems Sciences International*, **49** (2010), no. 4, 524 - 528.
http://dx.doi.org/10.1134/s1064230710040027

[11] A. V. Zubov, Stabilization of program motion and kinematic trajectories in dynamic systems in case of systems of direct and indirect control, *Automation and Remote Control*, **68** (2007), no. 3, 386 - 398.
http://dx.doi.org/10.1134/s0005117907030022

[12] A. V. Zubov, V. V. Dikusar, N. V. Zubov, Controllability criterion for

stationary systems, *Doklady Mathematics*, **81** (2010), no. 1, 6 - 7. http://dx.doi.org/10.1134/s1064562410010023

[13] I. V. Zubov, A. V. Zubov, The stability of motion of dynamic systems, *Doklady Mathematics*, **79** (2009), no. 1, 112 - 113. http://dx.doi.org/10.1134/s1064562409010347

[14] L. A. Bondarenko, A. V. Zubov, A. F. Zubova, S. V. Zubov, V. B. Orlov, Stability of quasilinear dynamic systems with after effect, *Biosciences Biotechnology Research Asia*, **12** (2015), 779 - 788. http://dx.doi.org/10.13005/bbra/1723

[15] A. V. Matrosov, G. N. Shirunov, Numerical-analytical computer modeling of a clamped isotropic thick plate, *2014 International Conference on Computer Technologies in Physical and Engineering Applications, ICCTPEA*, (2014), 1 - 96. http://dx.doi.org/10.1109/icctpea.2014.6893300

[16] S. A. Kabrits, V. F. Terent'ev, Numerical solution of one-dimensional nonlinear statics problems for elastic rods and shells in the presence of rigid constraits, *Soviet Applied Mechanics*, **20** (1984), 672 - 675. http://dx.doi.org/10.1007/BF00891729

[17] V. M. Malkov, S. A. Kabrits, Nonlinear Problems for a layer of low-compressible material, *Vestnik Sankt-Peterburgskogo Universiteta. Ser 1. Matematika Mekhanika Astronomiya*, **1** (1999), 86 - 91.

[18] J. Li, Y. Huang, W. Yang, Mathematical analysis and finite element simulation of a magnetized ferrite model, *Journal of Computational and Applied Mathematics*, **292** (2016), 279 - 291. http://dx.doi.org/10.1016/j.cam.2015.07.002

[19] H.M. Abdelali, R. Benamar, Non linear vibrations and bending stresses of symmetrically laminated composite skew plates , *International Journal of Applied Engineering Research*, **10** (2015), no. 15, 35272 - 35277.

[20] G. V. Alferov, O. A. Malafeyev, A. S. Maltseva, Programming the robot in tasks of inspection and interception, *International Conference on Mechanics - Seventh Polyakhov's Reading*, 2015, art. no. 7106713. http://dx.doi.org/10.1109/POLYAKHOV.2015.7106713

[21] Yu. M. Dal', Yu. G. Pronina, On concentrated forces and moments in an elastic half-plane, *Vestnik Sankt-Peterburgskogo Universiteta. Ser 1. Matematika Mekhanika Astronomiya*, **1** (1998), 57 - 60.

[22] Y. M. Dahl, Y. G. Pronina, Deformation of spherical pore in nonlinear-

elastic solid, *Bulletin of the Russian Academy of Sciences: Physics*, **70** (2006), no. 9, 1533 - 1535.

[23] P. Efimova, D. Shymanchuk, Dynamic model of space robot manipulator, *Applied Mathematical Sciences*, **9** (2015), no. 94, 4653 - 4659. http://dx.doi.org/10.12988/ams.2015.56429

[24] N. Fawazi, J.-Y. Lee, An improved energy based load-displacement prediction for slotted disc spring, *ARPN Journal of Engineering and Applied Sciences*, **11** (2016), no. 2, 837 - 840.

[25] K. Grari, J. Bouchnaif, M. Azizi, H. Fadil, A. Benslimane, Sensorless control of switched reluctance motor with fuzzy-PI controller, *Journal of Theoretical and Applied Information Technology*, **83** (2016), no. 1, 34 - 42.

[26] L.-L. Huang, G.-C. Wu, M.M. Rashidi, W.-H. Luo, Chaos analysis of the nonlinear duffing oscillators based on the new Adomian polynomials, *Journal of Nonlinear Science and Applications*, **9** (2016), no. 4, 1877 - 1881.

[27] S. A. Kabrits, L. V. Slepneva, Small nonsymmetric oscillations of viscoelastic damper under massive body action, *Vestnik Sankt-Peterburgskogo Universiteta. Ser 1. Matematika Mekhanika Astronomiya*, **2** (998), 78 - 85.

[28] K. Karthik Selva Kumar, L. A. Kumaraswamidhas, Investigation on vibration excitation behavior of an elastically mounted circular cylinder at different interference conditions, *International Journal of Applied Engineering Research*, **10** (2015), no. 24, 44315 - 44325.

[29] M. Nasirshoaibi, N. Mohammadi, Forced transverse vibration analysis of an elastically connected rectangular double-plate system with a Pasternak middle layer, *ARPN Journal of Engineering and Applied Sciences*, **10** (2015), no. 14, 6004 - 6013.

[30] M. L. Simonov, K. S. Zaitsev, N. P. Popova, The frequency response of a dynamic system, *Journal of Theoretical and Applied Information Technology*, **78** (2015), no. 3, 483 - 496.

[31] E. P. Kolpak, S. A. Kabrits, V. Bubalo, The follicle function and thyroid gland cancer, *Biology and Medicine*, **7** (2015), BM060.15.

[32] Y. E. Balykina, E. P. Kolpak, E. D. Kotina, Mathematical model of thyroid function, *Middle - East Journal of Scientific Research*, **19** (2014), 429 - 433.

[33] E. P. Kolpak, L. S. Maltseva, S. E. Ivanov, On the stability of compressed

plate, *Contemporary Engineering Sciences*, **8** (2015), no. 20, 933 - 942. http://dx.doi.org/10.12988/ces.2015.57213

[34] S. A. Kabrits, E. P. Kolpak, Numerical Study of Convergence of Nonlinear Models of the Theory of Shells with Thickness Decrease, *AIP Conference Proceedings*, **1648** (2015), 300005. http://dx.doi.org/10.1063/1.4912547

[35] E. P. Kolpak, L. S. Maltseva, Rubberlike membranes at inner pressure, *Contemporary Engineering Sciences*, **8** (2015), no. 36, 1731 - 1742. http://dx.doi.org/10.12988/ces.2015.510289

[36] S. E. Ivanov, V. G. Melnikov, On the two-dimensional nonlinear Korteweg - de Vries equation with cubic stream function, *Advanced Studies in Theoretical Physics*, **10** (2016), no 4, 157 - 165. http://dx.doi.org/10.12988/astp.2016.611

[37] S. E. Ivanov, V. G. Melnikov, Mathematical modeling vibration protection system for the motor of the boat, *Applied Mathematical Sciences*, **9** (2015), no. 19, 5951 - 5960. http://dx.doi.org/10.12988/ams.2015.58537

[38] E. P. Kolpak, S. E. Ivanov, Mathematical modeling of the system of drilling rig, *Contemporary Engineering Sciences*, **8** (2015), no. 16, 699 - 708. http://dx.doi.org/10.12988/ces.2015.55162

[39] Y. G. Pronina, Estimation of the life of an elastic tube under the action of a longitudinal force and pressure under uniform surface corrosion conditions, *Russian metallurgy (Metally)*, **2010** (2010), no. 4, 361 - 364. http://dx.doi.org/10.1134/S0036029510040208

[40] Y. G. Pronina, Lifetime assessment for an ideal elastoplastic thick-walled spherical member under general mechanochemical corrosion conditions, Computational Plasticity XII: Fundamentals and Applications - *Proceedings of the 12th International Conference on Computational Plasticity - Fundamentals and Applications*, COMPLAS 2013, 729-738.

[41] S. E. Ivanov, V. G. Melnikov, On the equation of fourth order with quadratic nonlinearity, *International Journal of Mathematical Analysis*, **9** (2015), no. 54, 2659 - 2666. http://dx.doi.org/10.12988/ijma.2015.510249

[42] E. P. Kolpak, S. E. Ivanov, Mathematical and computer modeling vibration protection system with damper, *Applied Mathematical Sciences*, **9** (2015), 3875 - 3885. http://dx.doi.org/10.12988/ams.2015.53270

**Received: March 13, 2016; Published: April 26, 2016**